RESEARCH ARTICLE

Analyzing the Effect of Mutual Inductance on the Grid Integrated Distributed Energy Sources: A Case Study of KEPCO Distribution Network

EHTISHAM ASGHAR[1], **SHAHID HUSSAIN**[2], **JUNG-SUNG PARK**[3],
YUN-SU KIM[1], **(Senior Member, IEEE), AND REYAZUR RASHID IRSHAD**[4]
[1]Graduate School of Energy Convergence, Gwangju Institute of Science and Technology (GIST), Gwangju 61005, South Korea
[2]Innovation Value Institue (IVI), School of Business, National University of Ireland Maynooth (NUIM), Maynooth, W23 F2H6 Ireland
[3]KEPCO Research Institute, Daejeon 34056, South Korea
[4]Department of Computer Science, College of Science and Arts, Najran University, Sharurah, Najran 68341, Saudi Arabia

Corresponding authors: Yun-Su Kim (yunsukim@gist.ac.kr) and Shahid Hussain (shahid.hussain@mu.ie)

ABSTRACT The intermittent power generation of Distributed Generators (DGs) poses significant challenges to the operation of the power grid. This intermittency, caused by the variable nature of renewable energy sources like solar and wind, leads to power flow imbalances and voltage fluctuations. Consequently, a thorough analysis of DGs integration, considering network contingencies, overloading concerns, and the thermal limits of substations, is essential for effective planning and managing the power grid to ensure seamless operation. Mutual Inductance (MI) analysis of distribution lines is essential for comprehending the behavior of the lines, loads, and DGs, as well as ensuring accurate modeling of the Distribution Network (DN). It enables the study of how changing currents in one conductor can induce voltages in nearby conductors, providing valuable insights for effective management and control of the distribution system. While the Korea Electric Power Corporation (KEPCO) currently does not emphasize mutual inductance-based power flow analysis, incorporating such analysis could provide valuable technical insights into the behavior of the power system, thereby potentially enhancing its operational efficiency and performance. In this paper, we analyzed the impact of MI on the DN and formulated the power flow problem. We calculated line impedance by taking into account the configuration of the overhead distribution line, the type of conductor used, and the frequency of the DN. Moreover, we developed a mathematical formulation, based on the backward-forward sweep power flow mechanism, to model polynomial ZIP loads and DGs, while considering both with and without MI cases. The proposed model is utilized with the backward-forward sweep power flow algorithm and applied to two case studies: the IEEE 34 bus test feeder and the KEPCO DN. The simulation results are evaluated by analyzing the voltage profile, system losses, voltage improvement, violations of nominal voltage limits, and voltage sensitivity, considering the temporal and spatial effects of loads and DGs inductions.

INDEX TERMS Mutual inductance, load modeling, power flow, bidirectional backward-forward power flow, voltage sensitivity analysis, distribution networks, distributed generations.

I. INTRODUCTION

The adoption of Distributed Generators (DGs) has gained momentum in recent years due to their advantages, including

The associate editor coordinating the review of this manuscript and approving it for publication was Fabio Mottola.

environmental friendliness and cost-effective electricity production [1]. However, their widespread integration at the distribution level poses several challenges for power grid operators, primarily stemming from the intermittent nature of DGs, which causes voltage fluctuations, network stability concerns, and reliability issues [2]. It necessitates an

understanding of the functional behavior of the power system in the presence of different types of loads and DGs. In this context, power flow analysis plays a significant role in characterizing the temporal behavior of the power system, making it applicable in network design, operational control, placement of DGs, and congestion control management.

In recent years, several iterative power flow algorithms [3], [4], such as Gauss-Seidel, Newton-Raphson (NR), and Fast Decoupled methods, have been extensively studied and applied in the literature for power system operation, planning, and control [5], [6], [7]. These algorithms are known for their simplicity and efficiency in solving high-voltage power networks with a low R/X ratio (where 'R' and 'X' represent the resistance and inductive reactance of distribution lines). However, when it comes to radial DNs characterized by a high R/X ratio, which fall into the category of ill-conditioned power systems [8], [9], these algorithms often struggle to provide solutions efficiently and may not converge reliably. Moreover, even the enhanced versions of the NR and Fast Decoupled methods encounter difficulties in achieving convergence for radial DNs with high R/X line ratios [9], [10]. A ladder network theory was employed in [11] to compute the power flow of a radial DN, resulting in quick convergence; however, it failed to achieve convergence in complex cases [12]. Another power flow method for radial DNs was presented in [13]; however, its scope is limited to nodal voltage magnitudes and does not cover the comprehensive studies required by distribution companies. The authors in [14] and [15] have developed a power flow algorithm based on bus injection-to-branch current and branch current-to-bus voltage matrices. While their method effectively analyzes power flow in small networks, it falls short in providing comprehensive coverage for large DNs [16]. In contrast, the voltage-dependent load power flow analysis algorithm proposed in [17] considers static load combinations and the parallel capacity of lines. This algorithm demonstrates justifiable and fast convergence when tested under various scenarios, including variable load conditions, different R/X ratios, and voltage levels. The Backward-Forward Sweep Power Flow (BFSPF) algorithm utilizes Kirchhoff's voltage law (KVL) and Kirchhoff's current law (KCL) to overcome limitations such as the singularity problem in transformer-connected modes and the requirement for a Jacobian matrix, which are encountered by the NR algorithm. The BFSPF algorithm serves as a powerful tool for power flow analysis in radial DNs. In a theoretical study conducted by the authors in [18], a power flow analysis was performed using BFSPF. However, further investigation is needed to understand the behavior of the network in the presence and absence of Mutual Inductance (MI). In the literature [12], [13], [14], [17], power flow analysis has been extensively conducted from different perspectives; however, a comprehensive comparison of various cases, including the presence of MI and without MI (WMI), has been overlooked, thereby neglecting the understanding of their impact on power flow results. For instance, the authors in [19]

presents a novel method for estimating mutual inductance and load resistance in a series-series compensated wireless power transfer system, enabling dynamic monitoring of coupling relationship and load conditions without receiver-side measurements, and demonstrating its effectiveness through experimental results, while this study [20] focuses on a small-scale dynamic wireless power transfer system for electric vehicles (EVs). It analyzes the dynamic mutual inductance between the coils due to misalignment, which significantly affects the charging process, including output power and overall efficiency. The study [21] investigates the mutual inductance between concentric planar spiral coils, analyzing the effects of track width and space between turns. Meanwhile, another study [22] presents a closed-form formula for the mutual inductance of coaxial hexagonal and octagonal planar spiral coils, validated through simulation and experimental fabrication on FR4 substrate, affirming the accuracy and feasibility of the proposed formulas. Line inductance plays a crucial role in determining the magnitude of the voltage profile and voltage sensitivity in a DN, and inaccurate voltage calculations can result in disturbances in real and reactive power flow, leading to power failures and potential damage to components [23]. In order to understand the operations of DNs with a significant penetration of distributed DGs, it is essential to incorporate accurate modeling of distribution lines and their loads, taking into account MI. However, the South Korean electric power company (KEPCO), considers the impact of MI on their DN with unidirectional power flow to be negligible and therefore does not include it in their power flow analysis. In contrast to the unidirectional conventional power system, the modern power system with the emergence of distributed generation supports bidirectional power flow and requires the consideration of proper mechanisms like MI to analyze and regulate the power flow [23]. Furthermore, previous studies that primarily focused on the Gauss-Seidel, Newton-Raphson, and Fast Decoupled methods have largely overlooked the consequences of considering MI in power flow analysis. This study aims to address this knowledge gap by examining the impact of MI (both with MI and without MI) on a DN with varying penetration ratios of DGs. Additionally, a case study is conducted on the KEPCO DN to evaluate the potential effects of MI on its operation. Various scenarios, including the presence of MI, absence/without of WMI, different penetration ratios of DGs, and loads, are simulated. The KEPCO DN is comprised of distribution lines connected to DGs such as photovoltaics (PVs) and wind turbines (WTs) with ACSR/AW conductors, along with ZIP (constant impedance (Z), current (I), and power (P)) loads [23]. Our contribution in this work is summarized as follows:

- We calculated a precise line impedance, considering the parameters of overhead distribution lines, conductor type, and KEPCO DN frequency. We incorporate polynomial ZIP load and DG models, accurately capturing the non-linear behavior of loads and the impact of distributed generation sources. The inclusion of both MI

and WMI cases allows us to account for the mutual coupling effects, such that the MI case considers the mutual coupling between adjacent line conductors, while the WMI case analyzes the system without considering the mutual coupling effects.

- We formulate the power flow problem by considering a radial DN to analyze the impact of MI and WMI under various load conditions and penetration levels of DGs. Furthermore, we employ the BFSPF algorithm to solve the power flow problem and ensure accurate line impedance estimation, considering the effects of loads, DGs, and mutual coupling. This approach leads to a comprehensive analysis of the system's behavior in terms of voltage sensitivity and node voltage profiles across different DG penetration levels.
- We performed two case studies using the BFSPF algorithm on the IEEE 34 bus test feeder and the KEPCO DN system. The simulation results were analyzed and evaluated based on several criteria, including voltage profile, system losses, voltage improvement, violations of nominal voltage limits, and the sensitivity of voltage to temporal and spatial variations in loads and DGs.

The paper is organized as follows: Section II presents the system modeling for the IEEE 34 bus test feeder and the KEPCO DN system. Section III provides a detailed explanation of the developed algorithm's mechanism, including the pseudocode. Section IV focuses on voltage sensitivity analysis, examining the impact of temporal and spatial load and DG variations on voltage profiles. Section V discusses the simulation results, including voltage profiles, system losses, improvements, and violations of voltage limits. Finally, Section VI provides a concise conclusion summarizing the key findings and suggesting future research directions.

II. SYSTEM MODELING
The power flow analysis is conducted by considering a distributed network system that consists of loads, lines, and DGs. A schematic diagram of a typical DN is illustrated in Figure 1, and the details of the functional components are presented in this section.

A. THE LOAD MODEL OF DISTRIBUTED NETWORK
In conventional DNs, power flows unidirectionally from generation to the consumption side. However, the current power system enables bidirectional power flow in both upstream and downstream directions, facilitating the incorporation of prosumers, such as microgrids and Electric Vehicles (EVs) [24], [25]. This paradigm shift presents opportunities for peak load shaving, enhanced voltage stability, and the provision of ancillary services. However, it also poses challenges related to the efficient integration of DGs and effective management of prosumers within the power system [26], [27]. The dynamic and uncertain behavior of DGs and prosumers necessitates the application of diverse techniques and algorithms for seamless integration [28], [29], [30], [31]. In academic studies, the steady-state mode of DNs is
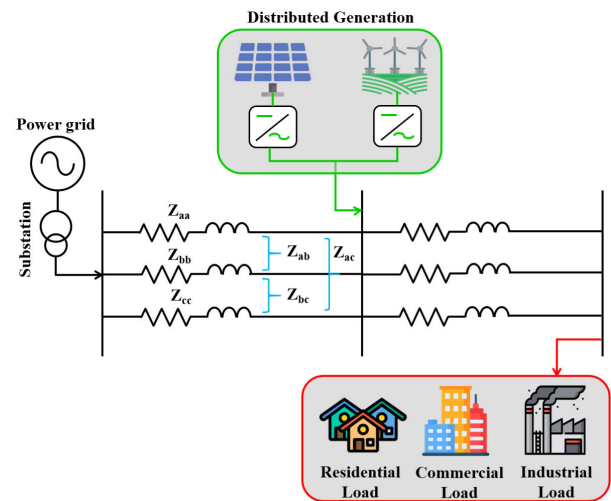

FIGURE 1. A schematic diagram of typical distribution network system comprising of distributed generations and different types of loads.

commonly analyzed. In sequel, this work aims to understand the functional behavior of DNs by analyzing their steady-state mode. In sequel, this work aims to comprehend the functional behavior of DNs by analyzing their steady-state mode. In this study, we consider the Constant Active and Reactive Power (CP&Q) and Polynomial ZIP types of static load models.

B. THE ZIP LOAD MODEL
In practical scenarios, the power system encompasses diverse loads that exhibit temporal variations. Typically, a node in the power system consists of three types of loads: residential, commercial, and industrial, as depicted in Figure 1. The distribution of these load types varies depending on the day of the week, distinguishing between weekdays and weekends [32]. The ZIP load model is a well-established mathematical framework used to accurately represent power consumption in electrical networks. It is particularly useful in characterizing the behavior of loads based on the voltage at a specific node, as well as the active and reactive power levels. The ZIP load model comprises three distinct components, namely constant impedance (Z), constant current (I), and constant power (P) loads. These components capture different aspects of load behavior and allow for a comprehensive description of the load characteristics. To express the ZIP load model mathematically, we can utilize equations (1) and (2) as follows:

$$P = \alpha_{Z_p} P_o V^2 + \alpha_{I_p} P_o V + \alpha_{P_p} P_o \quad (1)$$

$$Q = \alpha_{Z_q} Q_o V^2 + \alpha_{I_q} Q_o V + \alpha_{P_q} Q_o \quad (2)$$

In these equations, the α_{Z_p} and α_{Z_q} are the contribution factors represent the percentage of the reference power (P_o) and reference reactive power (Q_o), respectively, that depend on the square of the voltage (V^2) due to the constant impedance (Z) load component. They characterize the impact

of the impedance-related effects of the load on both active power (P) and reactive power (Q). The terms α_{I_p} and α_{I_q} are the contribution factors signify the percentage of the reference active power (P_o) and reference reactive power (Q_o), respectively, that are directly proportional to the voltage (V) due to the constant current (I) load component. They capture the active power and reactive power contributions associated with the current-related effects of the load. Likewise, the terms α_{P_p} and α_{P_q} are the contribution factors represent the percentage of the reference active power (P_o) and reference reactive power (Q_o), respectively, that remain constant regardless of the voltage (V) due to the constant power (P) load component. They represent the portions of the active power and reactive power that remain constant irrespective of the voltage fluctuations.

C. THE DISTRIBUTION LINES
In general, distribution lines are categorized into Medium Voltage (MV) and Low Voltage (LV) based on their voltage levels, which vary between countries such as the United States (US), Europe (EU), and Asia (specifically South Korea). For instance, in the United States, Europe, and Asia (specifically South Korea), typical MV and LV DNs operate at voltage levels of 13 kV and 0.48 kV (US), 20 kV and 0.4 kV (EU), and 22.9 kV and 0.38 kV (Asia-South Korea) respectively [33], [34]. The line models for these distribution networks are designed to incorporate the self-impedance (Z_{ii}) and mutual impedance (Z_{ij}) between the same and other lines, as illustrated in Figure 2. These impedance values are of significant importance for the analysis and modeling of distribution lines in various countries. In the case of KEPCO (South Korea), detailed information regarding these impedance values is presented in the following sub-sections.

1) IMPEDANCE CALCULATION FOR KEPCO DLs
In this study, we utilize the KEPCO standard Aluminium Conductors, Aluminium Clad Steel Reinforced (ACSR/AW) configuration for computing the self and mutual impedance of Distribution Lines (DLs). This configuration consists of outer aluminum layers and inner strands composed of both aluminum and aluminum-clad steel. The specific parameters for this conductor, which are provided in Table 1, are used to represent the impedance of three-phase DLs through a 3×3 matrix [35]. The self and mutual impedances are computed using Carson's equation, which takes into account the gaps between the three phases (a, b, and c), the network frequency, the Geometric Mean Radius (GMR), resistance, and conductor radius as described in equations (4)-(13) [36]. The terms GMR_i and D_{xy} represent the geometric mean radius for the i-th conductor (equation (6)) and the distance between the strands of the conductor, respectively. The parameter d_{ij} indicates the distance between phases a, b, and c, in each case. In the KEPCO distribution network, an overhead configuration is employed for the distribution lines, with a standardized

TABLE 1. The Parameters of luminium Conductors, Aluminium Clad Steel Reinforced/Aluminium Wires.

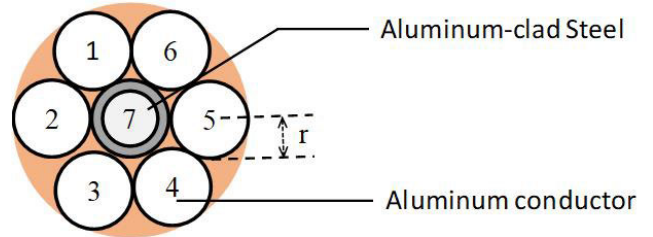| Nominal Cross Sectional Area (mm²)	No. and Dia. of of Strands (No/mm)		Electric Resistance (ohm/km, 20 C)
	Al	Aw	
58	6/3.5	1/3.5	0.47100

FIGURE 2. An overview of the Aluminium Conductors, Aluminium Clad Steel Reinforced/Aluminium Wires with seven strands.

spacing of 1720 mm and 560 mm between phases a, b, and b, c, respectively, as depicted in Figure 3. Based on the overhead configuration of the Distribution Lines (DLs), along with the provided parameters and equations (4)-(13), we have computed the self and mutual impedances.

$$Z_{dl} = \begin{bmatrix} Z_{aa} & Z_{ab} & Z_{ac} \\ Z_{ba} & Z_{bb} & Z_{bc} \\ Z_{ca} & Z_{cb} & Z_{cc} \end{bmatrix} \tag{3}$$

$$Z_{ii} = r_i + \alpha\left[\frac{f}{60}\right] + j\beta\left[\frac{f}{60}\right]\left[ln\frac{1}{GMR_i} + \gamma\right] \Omega/km \tag{4}$$

$$Z_{ij} = \alpha\left[\frac{f}{60}\right] + j\beta\left[\frac{f}{60}\right]\left[ln\frac{1}{d_{ij}} + \gamma\right]\Omega/km \tag{5}$$

$$GMR_i = \sqrt[7\times7]{(X)^6(Y)} \tag{6}$$

$$X = D_{11}D_{12}D_{13}D_{14}D_{15}D_{16}D_{17} \tag{7}$$

$$Y = D_{71}D_{72}D_{73}D_{74}D_{75}D_{76} \tag{8}$$

$$D_{14} = 4r \tag{9}$$

$$D_{11} = D_{77} = r \tag{10}$$

$$D_{13} = D_{15} = 2\sqrt{3}r \tag{11}$$

$$D_{12} = D_{16} = D_{17} = 2r \tag{12}$$

$$D_{ij} = 2r \quad i = 7, \ \forall j = 1, 2, \ldots, 6 \tag{13}$$

where $\alpha = 0.05919$, $\beta = 0.07537$, and $\gamma = 6.7458$, $Z_{ii} = 0.8538 + j1.4106$, $Z_{ab} = Z_{ba} = 0.0953 + j0.75298$, $Z_{ac} = Z_{ca} = 0.0953 + j0.7187$, and $Z_{bc} = Z_{cb} = 0.0953 + j0.8890 \ \Omega/mi$.

2) THE DISTRIBUTED GENERATORS
Traditional power systems are characterized by centralized power generation, where power flows in a unidirectional

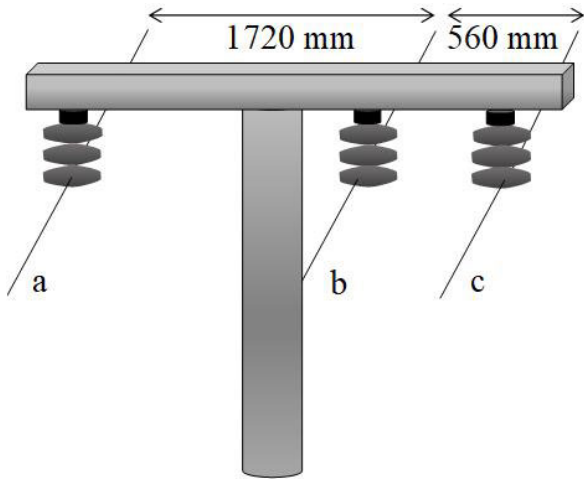**FIGURE 3.** A representation of the overhead line configuration according to the Korea Electric Power Company (KEPCO) standard.

FIGURE 4. Illustration of voltage as function of load and PV penetration in time.

manner from generation sources to end users However, the environmental unsustainability of centralized power generation technologies, including coal, oil, and gas, has led to heightened global awareness regarding issues such as global warming and energy crises. This has consequently spurred a widespread shift towards the utilization of more sustainable energy sources, particularly the advancement of DGs such as wind WTs and PVs, as well as the emergence of prosumers integrating Energy Storage Systems (ESSs) and EVs [37], [38], [39]. The integration of PVs, WTs, ESSs, and EVs into the power system typically involves the use of dedicated power-electronic interfaces, also known as converters, as illustrated in Figure 1. Depending on the control mechanism employed by the converters, the DGs can be integrated into the DNs as either PQ (active and reactive power control) or PV (active power control) nodes [40]. Integrating DGs offers numerous benefits such as low-cost power generation, environmental friendliness, and reduced power losses. However, the integration of DGs also poses challenges such as managing the upstream power flow, addressing network instability due to time-varying power injections into DN, and the potential impact on both the DN and utility operators, as illustrated in Figure 4, which shows the influence of DGs on DN voltage and is discussed in the following.

- *Voltage vs load:* As the load increases, the voltage in the distribution network tends to decrease due to the voltage drop across network components caused by the higher current flow. Maintaining appropriate voltage levels is crucial for ensuring reliable power supply and proper functioning of electrical equipment.
- *Voltage vs DGs:* The voltage in the distribution network increases proportionally with the penetration level of PV systems, as they contribute power to the grid. This direct relationship between voltage and DGs like PVs highlights that higher levels of PV integration result in higher voltage levels in the network.
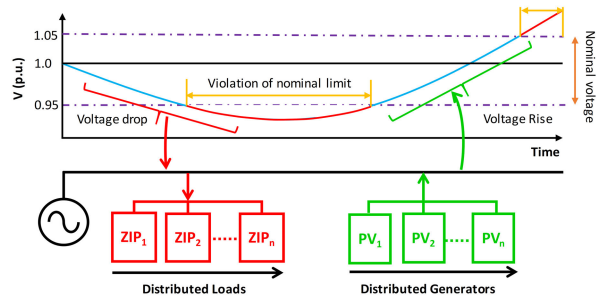
It is evident that in both cases, once the load and DGs penetrations exceed a certain threshold, boundary constraints are violated. This underscores the importance of load induction control and effective DGs management, emphasizing the need for comprehensive load power flow analysis to understand the behavior of DNs under diverse load and DGs penetration scenarios.

III. BACKWARD FORWARD SWEEP POWER FLOW METHOD FOR ANALYZING THE LOAD FLOW OF THE DISTRIBUTION NETWORK

The backward-forward sweep power flow method is a robust computational technique widely employed for load flow analysis in radial DNs. It encompasses an iterative process that incorporates two crucial computational steps, meticulously executed at each iteration, to accurately determine the power flow behavior within the network [41]. In this study, we implemented the BFSPF method to calculate the power flow for all three phases of the distribution power system. Specifically, considering the single-source radial distribution network illustrated in Figure 5, the BFSPF method performs the following two steps to accurately determine the power flow behavior within the network.

A. THE BACKWARD SWEEP MECHANISM FOR ANALYZING THE NODAL POWER FROM END NODE

In this step of the algorithm, the backward sweep commences by traversing the connected branches in a reverse direction, initiating from the last node and progressing backward through each subsequent node. At each iteration, the algorithm determines the current by utilizing the updated voltage values obtained from the preceding iteration while propagating in the backward direction [42]. During the backward sweep step, the load at a specific node n is updated using Equation (14), followed by the computation of the overall current by combining the currents of the b connected branches using Equation (15).

$$I_{an}^k = \left[\frac{(A + B + C) + j(D + E + F)}{V_{an}^{k-1}} \right]^* \quad (14)$$

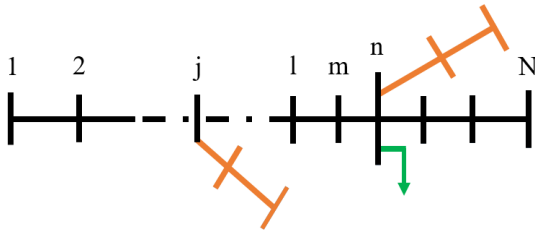$$I_{amn}^k = I_{an}^k + \sum_{b \in B} I_b^k \quad (15)$$

FIGURE 5. Visualization of Single Line Radial Distribution Feeder Network Topology.

where $A = \alpha_Z P_o (V_{aj}^{k-1})^2$, $B = \alpha_I P_o V_{aj}^{k-1}$, $C = \alpha_P P_o$, $D = \alpha_Z Q_o (V_{aj}^{k-1})^2$, $E = \alpha_I Q_o V_{aj}^{k-1}$, $F = \alpha_Q Q_o$, I_{amn}: current of branch mn, I_{an}: nodal current at bus n, and I_b: branch current emanated from bus n.

B. THE FORWARD SWEEP MECHANISM FOR ANALYZING THE NODAL POWER FLOW FROM THE SOURCE NODE

The forward sweep step initiates from the feeder/source node and progresses forward to determine the voltage drop by utilizing the current computed in the previous step. In this step, the source node voltage is maintained at a constant value of 1 per unit (p.u.) [43]. Referring to Figure 5, the voltage at node n is computed by considering the known voltage at node m and the voltage drop ($I_{mn} Z_{mn}$) across the branch connecting nodes m and n, as per Equation (16). The impedance and current corresponding to the voltage drop can be calculated for each phase using their respective matrices, as described by Equations (17) and (18).

$$V_{an}^k = V_{am}^k - Z_{mn} I_{mn}^k \tag{16}$$

$$Z_{mn} = \begin{bmatrix} Z_{mn}^{aa} & Z_{mn}^{ab} & Z_{mn}^{ac} \\ Z_{mn}^{ba} & Z_{mn}^{bb} & Z_{mn}^{bc} \\ Z_{mn}^{ca} & Z_{mn}^{cb} & Z_{mn}^{cc} \end{bmatrix} \tag{17}$$

$$I_{mn} = \begin{bmatrix} I_{amn} \\ I_{bmn} \\ I_{amn} \end{bmatrix} \tag{18}$$

where V_n: Voltage at node n, V_m: Voltage at node m, and Z_{mn}: Line impedance of branch mn, current matrices for each of the three phases connecting the two nodes m and n.

C. PSEUDOCODE OF THE POWER FLOW ALGORITHM FOR ANALYZING THE IMPACT OF THE MUTUAL INDUCTANCE

The following pseudocode represents the power flow algorithm designed to analyze the effects of mutual inductance on the three-phase DN, illustrated in Figure 5. This algorithm takes inputs including active power, reactive power, and line data. It then executes the backward and forward sweep computational steps to compute the voltage profile, line losses, and nodal voltage sensitivity. The main steps of the algorithm are described in detail below.

Step 1. Initialize all the system parameters, including the initial voltage with 1 p.u. and the phases ($a = 0°$, $b = -120°$, and $c = 120°$) for all the nodes.

Step 2. Calculate the active and reactive power, along with the current, for each node using Equations (1) to (4), which are implemented in lines 3 to 6 of the algorithm.

Step 3. Execute the backward sweep process from lines 8 to 16 to analyze the nodal and all the branches (lines) power flow, starting from the end node, utilizing Equations (14) and (15).

Step 4. Perform the forward sweep process from lines 17 to 20 to compute the voltages for each node and their corresponding branches (lines), starting from the source node, as defined by Equation (16) to (18).

Step 5. Get the maximum voltage deviation in line 21.

Step 6. Check the convergence of the error against ϵ to determine if convergence has been achieved. If convergence has not been reached, proceed to line 3 and repeat the entire process until convergence is achieved.

Step 7. Once the error converged print the voltage and line losses.

IV. VOLTAGE SENSITIVITY ANALYSIS
A. THE NEWTON RAPHSON METHOD FOR VOLTAGE SENSITIVITY

Voltage Sensitivity Analysis (VSA) is a procedure that captures the bus voltage status as it varies over time in response to changes in power, enabling the inference of voltage changes based on complex power variations [44]. This inference is achieved by constructing a voltage sensitivity matrix, which correlates voltage changes with variations in complex power, using the widely employed conventional approach of the Newton-Raphson (NR) method for VSA [45]. To analyze the voltage sensitivity using the NR method, let us consider a distribution network comprising N buses, where the active and reactive power are denoted as P_j and Q_j, respectively, and the voltage change is represented as ΔV_k for buses $j, k \in N$. In particular, we will examine the voltage sensitivity of a single bus when its power varies, i.e., considering the case where $k = j$. In the Newton-Raphson (NR) method, the variables P_j, Q_j, and voltage ΔV_k are interconnected through a system of nonlinear equations, which are typically solved using the Jacobian matrix approximation [46]. However, it is important to note that the computational time of the NR method is directly proportional to the size of the network. As the number of network buses increases in large DNs, the computational time of the NR method grows linearly with the size of the network, making it computationally expensive and impractical to implement [47]. This necessitates the development of new VSA techniques that are more generic and capable of efficiently handling network changes while reducing computational complexity.

Algorithm 1 Power Flow for Analyzing the MI

Input: Line length, line type, line impedance, active power and reactive power
Output: Node voltage and line losses

 1: Initialize system parameters
 2: **while** $(i \leq |N|)$ **do**
 3:      **for** $j \leftarrow 1$ *to* $|N|$ **do**
 4:          Compute P_L ▷ *According to Eq.* (1)
 5:          Compute Q_L ▷ *According to Eq.* (2)
 6:          $N_I[j] \leftarrow \left(\frac{P_L[j] + Q_L[j]}{V[j]}\right)$
 7:      **end for**
 8:      **for** $m \leftarrow |N|$ to 1 **do**   ▷ *Backward process*
 9:          **if** $(N[m] == 0)$ **then**
10:              $N_I[m] \leftarrow N_I[m]$
11:          **else if** $(N[m] == 1)$ **then**
12:              $N_I[m] \leftarrow N_I[m] + B_I$
13:          **else if** $(N[m] == 2)$ **then**
14:              $N_I[m] \leftarrow N_{I[m]} + B_I + B_I'$
15:          **end if**
16:      **end for**
17:      **for** $n \leftarrow 1$ to $|N|$ **do**   ▷ *Forward process*
18:          $N_V[n] \leftarrow N_V[n-1] - (N_Z \times N_I)$
19:          $E_V[n] \leftarrow N_V[n] - N_V[n-1]$
20:      **end for**
21:      $E_{max} \leftarrow \max(E[n])$ ▷ *Get maximum error*
22:      **if** $(E_{max} \geq \epsilon)$ **then**
23:          Go to Step 3
24:      **else**
25:          Print $V[i]$ and $L[i]$
26: $i \leftarrow i + 1$
27:      **end if**
28: **end while**

B. THE PROPOSED MUTUAL INDUCTANCE BASED VSA

In contrast to the NR method, the proposed approach utilizes linear equations for convergence, eliminating the need for computationally intensive inverse computations of the complex Jacobian matrix to determine the magnitude of voltage variation at the target bus. This achievement is made possible by leveraging the inherent flexibility of the BFSFP algorithm, allowing it to effectively adapt to network modifications. Consequently, we can apply the BFSFP algorithm to perform VSA on a three-phase radial DN. By employing the BFSFP mechanism, we can efficiently search for the minimum number of connections between nodes, enabling precise VSA calculations based on mutual inductance. As a result, this approach offers a reduced computational cost and a smaller memory footprint compared to the NR method. It is worth noting that the voltage sensitivity is strongly influenced by the power flow in all three phases and the impedance (including self and mutual impedance). Therefore, any changes in power or impedance directly impact the voltage sensitivity.

TABLE 2. The assumption of percentage contribution factors for the ZIP based on the KEPCO network [48].

Active Power		Reactive Power	
α_{Z_p}	0.35	α_{Z_q}	0.56
α_{I_p}	0.13	α_{I_q}	0.08
α_{P_p}	0.52	α_{P_q}	0.36
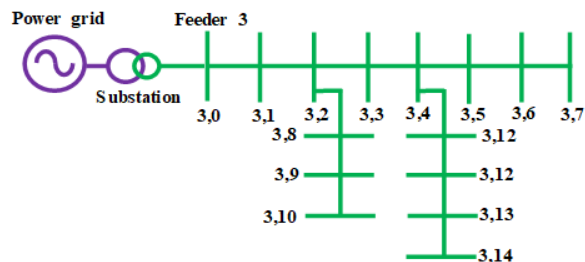
FIGURE 6. A representation of the KEPCO radial network topology [50].

V. SIMULATION SETUP AND RESULTS DISCUSSION

The BFSPF algorithm is utilized for the analysis of two radial Distribution Networks (DNs): the IEEE 34 bus DN, which operates at a voltage level of 24.9 kV with a total power capacity of 2500 kVA [49], and the KEPCO DN with a voltage level of 22.9 kV and a total power capacity of 100 MVA (Figure 6) [50]. The IEEE 34 bus topology comprises a mix of single-phase lines (Figure 7) and three-phase lines, accommodating 6 spot loads and 27 distributed loads [51]. The slack bus, labeled, as bus 800, serves as the connection point to the upstream power transmission network. Multiple case studies were conducted to analyze the power flow and Voltage Sensitivity Analysis (VSA) based on mutual inductance for both topologies. The base case was modeled with a total active power of 1319 kW and a reactive power of 819 kVAR. The percentage contribution factors, denoted as $\alpha_{Z_p}, \alpha_{I_p}, \alpha_{P_p}, \alpha_{Z_q}, \alpha_{I_q},$ and α_{P_q}, representing the ZIP model, were assumed based on the KEPCO standard DN obtained from the KEPCO network [48] and are listed in Table 2. It should be noted that in the subsequent analysis, we have given due consideration to the lines of different phases - a, b, and c - as it is evident that maintaining a proper balance within a specified range is a fundamental regulatory requirement [52]. This balance is crucial for ensuring the stability and reliability of the distribution system. Therefore, we have adhered to a well-established practice of preventing the current flow in phases a, b, and c from being opposite to each other [53], [54].

A. RESULTS FOR THE IEEE 34 BUS SYSTEM
1) CP&Q LOAD WITH AND WMI

In this analysis, a constant active and reactive power load model (CP&Q) was considered to calculate the power flow in the DN. The impact of mutual inductance (MI) on the load flow was further investigated by considering two scenarios: (1) CP&Q with MI, and (2) CP&Q without MI. The voltage
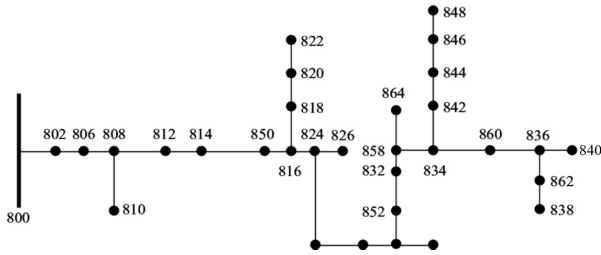
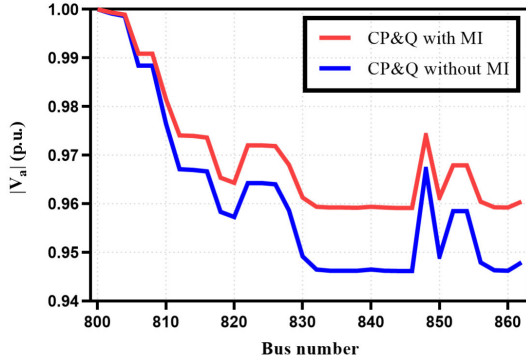**FIGURE 7.** Modified layout of the IEEE 34 single line bus system.

FIGURE 8. A comparison of the voltage profile with-MI and without-MI (WMI) for the IEEE 34 bus system.

FIGURE 9. A comparison of voltage profile of the ZIP load using with-MI and WMI for the IEEE bus 34 system.

FIGURE 10. A comparison of the voltage profile in WMI case for the IEEE 34 bus system.

FIGURE 11. A comparison of the active power loses in branches in WMI case for the IEEE 34 bus system.

profiles for each of the two cases are shown in Figure 8. It can be observed that in both cases, there is a voltage drop across the nodes based on their respective loads. However, there is a notable difference in the behavior of the voltage drop between the two cases.

2) ZIP LOAD WITH MI AND WMI

In this case, a more realistic scenario of power flow was conducted by incorporating the ZIP load model in the DN. Two cases were considered: (1) ZIP with MI, and (2) ZIP without MI. The results for the DN are illustrated in Figure 9. In case (1), the lowest node voltage from node 830 to 850 is well above 0.96 p.u., while in case (2), the lowest node voltage for these nodes is approximately 0.95 p.u. This indicates that the ZIP with MI case leads to further improvement in voltage compared to case (1) of the previous scenario (CP&Q).

3) ZIP AND CP&Q LOADS WMI

In this case, the power flow was computed for two load models: CP&Q and ZIP, without considering the effect of MI. The results for the node voltage and line losses (active power losses) are presented in Figure 10 and Figure 11, respectively. It can be observed that the voltage profiles gradually decrease, particularly from node 832 to 848, where they drop below 0.95 p.u. Regarding the line losses, the CP&Q without MI case corresponds to higher losses compared to the ZIP without MI case. This indicates that the CP&Q case requires more power supplies to compensate for the power losses.
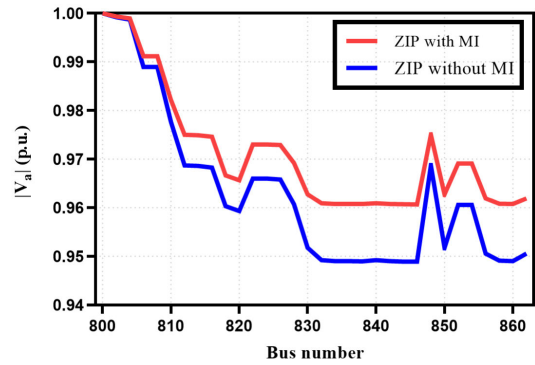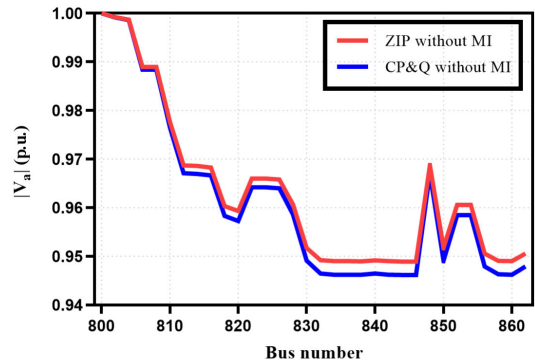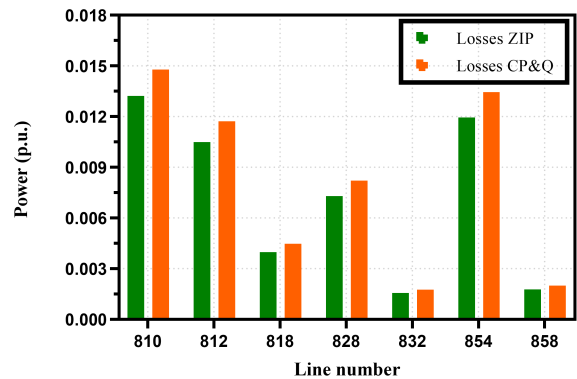
4) ZIP AND CP&Q LOADS WITH MI

The previous analysis demonstrates that the ZIP load model significantly contributes to voltage improvement and helps in minimizing losses. Consequently, a more comprehensive analysis is conducted for the ZIP and CP&Q load models in conjunction with MI, and the corresponding results for voltage and line losses are depicted in Figure 12 and Figure 13, respectively. From Figure 12, it can be observed that the voltage profile is significantly improved compared to the previous case (WMI). In this scenario, the lowest voltage
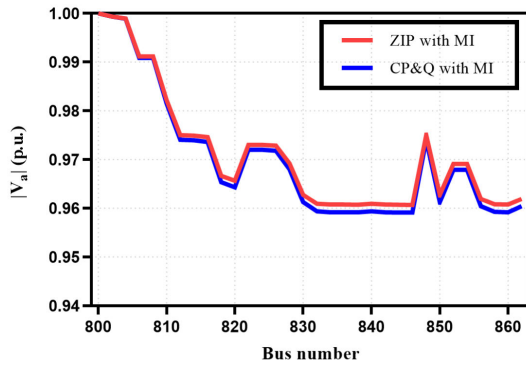
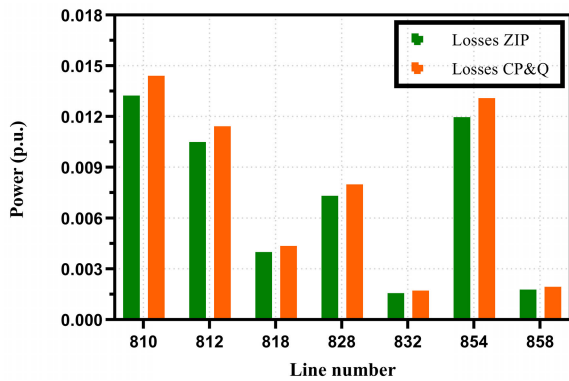**FIGURE 12.** A comparison of the voltage profile with MI case for the IEEE 34 bus system.

FIGURE 13. A comparison of the active power loses in branches with MI case for the IEEE 34 bus system.

FIGURE 14. A comparison of the voltage profile with-MI without MI for the KEPCO DN.
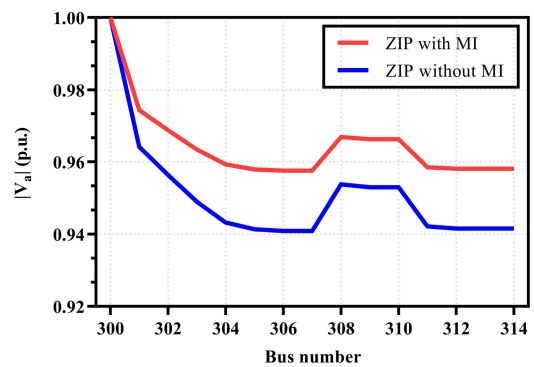
FIGURE 15. A comparison of the voltage profile with-MI and WMI for the KEPCO DN.

level is increased from below 0.95 p.u. to above 0.96 p.u., indicating that the incorporation of MI-based analysis effectively maintains the voltage level well above 0.95 p.u. and close to 1 p.u. The improvement in voltage with the ZIP load model can be attributed to the direct relationship between voltage and ZIP. As the voltage decreases, the ZIP load also decreases, resulting in a reduced voltage drop in the distribution lines. Furthermore, in this case, a further reduction in line losses is observed compared to the WMI case, as illustrated in Figure 13.

B. SIMULATION RESULTS DISCUSSION FOR KEPCO DN
1) CP&Q LOAD WITH AND WMI
In this case, the CP&Q load model is considered to analyze the impact of MI with two scenarios: with-MI and WMI, as shown in Figure 14. From the figure, it can be observed that the minimum voltages are 0.94 p.u. and 0.96 p.u. for the with-MI and WMI cases, respectively.

2) ZIP LOAD WITH AND WMI
In this case, the load model is modified to incorporate ZIP load, which represents a more realistic situation. The impact of MI is then analyzed using two different scenarios, as depicted in Figure 15. Upon examination of the figure, a slight difference can be observed in the minimum voltage between the with-MI and WMI cases. However, the average voltage remains the same for both scenarios.
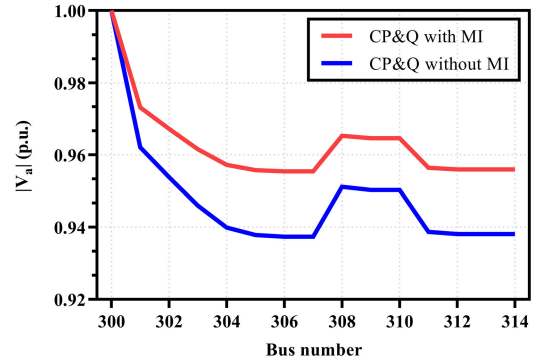
3) ZIP AND CP&Q LOADS WMI
In this case, we consider two load models, namely ZIP and CP&Q, without considering the presence of MI. The performance of the ZIP load model is observed to be better compared to the CP&Q load model, as depicted in Figure 16. The minimum voltage under the ZIP load model is measured to be 0.938 p.u., while the minimum voltage under the CP&Q load model is recorded as 0.942 p.u.

4) ZIP AND CP&Q LOADS WITH MI
Furthermore, we conducted tests on the KEPCO DN to analyze the voltage profile considering the ZIP and CP&Q load models with the presence of MI. A comparison of these load models in the *with MI* case is illustrated in Figure 17. It is noteworthy that the presence of MI equally contributed to the improvement of the voltage profile for both the ZIP and CP&Q load models.

C. INTEGRATION OF DGs WITH THE KEPCO DN
1) ZIP LOAD WITH AND WMI
The rapid development of renewable energy technology has led to an increasing trend in the integration of DGs into power systems. However, the intermittent nature of DGs introduces fluctuations in power grid stability, necessitating power flow analysis to assess the impact of DG penetration and enable effective control strategies.
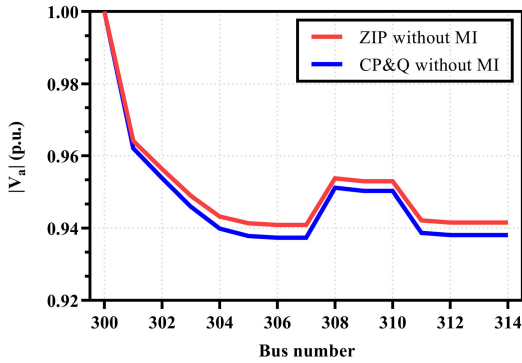
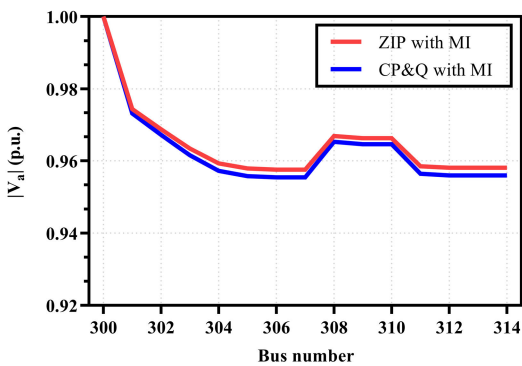**FIGURE 16.** A comparison of the voltage profile WMI case for the KEPCO DN.

FIGURE 17. A comparison of the voltage profile with MI case for the KEPCO DN.

FIGURE 18. A comparison of the voltage profile with MI and with MI & DG for the KEPCO DN.

FIGURE 19. A comparison of the voltage profile of ZIP load induction with the different penetration level of DGs for the KEPCO DN.

As anticipated, the integration of DGs has a significant impact on the network voltage, as shown in Figure 18. The voltage levels are consistently above the lower threshold, typically ranging from 0.90 to 0.95 p.u., with only slight variations. Furthermore, the figure illustrates that in the *"ZIP with MI"* case, the lowest node voltage is approximately 0.95 p.u., and the average voltage is around 0.96 p.u. On the other hand, in the *"ZIP with MI and DG"* case, the lowest and average voltages are approximately 0.97 p.u. and 0.98 p.u., respectively.

2) ZIP LOAD WITH MI AND DIFFERENT DG PENETRATION LEVELS

To further examine the impact of DGs, we conducted an analysis by varying the DG penetration level from 0% to 100%. The results, depicted in Figure 19, illustrate the voltage profile at different penetration levels (0%, 25%, 50%, 75%, and 100%) under the *"ZIP with MI"* case. The figure clearly demonstrates the relationship between DG penetration and the voltage profile, particularly at higher penetration levels. As the DG penetration increases, the voltage profile tends to approach 1 p.u., indicating a more stable voltage condition in the system. It is important to note that the results are specific to the selected bus located approximately 14 km from the slack bus. The trends observed in the voltage profile may vary for different bus locations within the network.
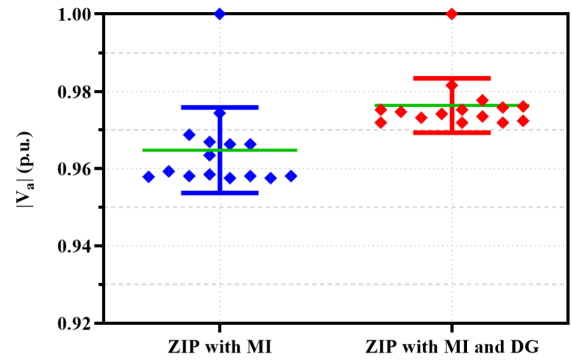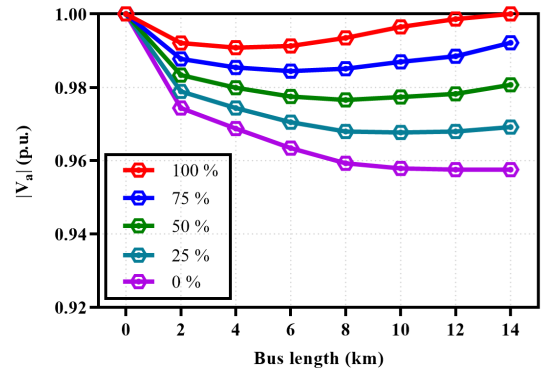
D. ANALYSIS FOR THE IDENTIFICATION OF THE MOST SENSITIVE NODES

To assess the impact of load models, MI, and DG integration, we conducted a comprehensive analysis using the *"CP&Q and ZIP load WMI"* and *"CP&Q and ZIP load with MI"* scenarios. The objective was to identify the most sensitive nodes in the KEPCO DN. By comparing these scenarios, we aimed to determine the nodes that exhibit significant changes in response to variations in load models, the presence of mutual inductance, and DG integration. This analysis provides valuable insights into the nodes that require careful monitoring and potential optimization strategies to enhance system performance and voltage stability.

1) NODE SENSITIVITY WITH CP&Q AND ZIP LOADS WMI

In this case study, we examined the sensitivity of bus number 14 to variations in active power. The active power of this bus was systematically varied in the range of 0-100 kW, with a step size of 10 kW, capturing both positive and negative power flow directions. The positive power flow represents increasing load, while the negative power flow represents DG power injection. Given the sensitive relationship between voltage and power, any change in power has an impact on all phases. To analyze the node voltage sensitivity, we considered the CP&Q and ZIP load models, specifically focusing on power changes in phase *"a"*. The results, depicted in Figure 20, illustrate the voltage variations for both cases
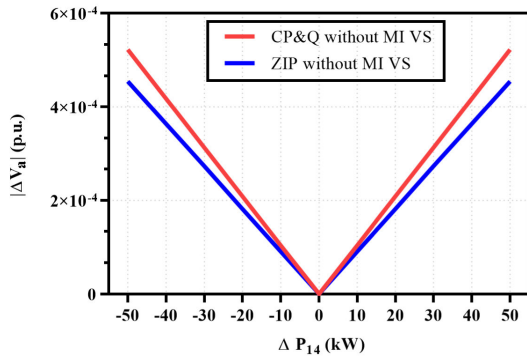
FIGURE 20. A comparison of the voltage sensitivity WMI case for the KEPCO DN.

FIGURE 21. A comparison of the voltage sensitivity with MI case for the KEPCO DN.

FIGURE 22. A comparison of the voltage sensitivity of all nodes with MI case for the KEPCO DN.

without considering MI. From the figure, it is evident that the node exhibits higher sensitivity to power changes in the CP&Q case, resulting in more significant variations in the voltage profile compared to the ZIP case. This finding highlights the importance of load models in understanding voltage sensitivity and supports the potential for optimizing the system by leveraging different load models.

2) NODE SENSITIVITY WITH CP&Q AND ZIP LOADS WITH MI

In this case, we kept all the settings from the previous scenario except for the inclusion of MI. The output results are depicted in Figure 21, revealing a notable disparity in the voltage sensitivity profile compared to the *"CP&Q and ZIP load WMI"* case. The introduction of MI into the analysis significantly alters the voltage sensitivity characteristics. This is because the ZIP load model is more nonlinear than the constant *CP&Q* load models, meaning that the relationship between changes in the node voltage and changes in the load is not as proportional as it is in the constant *CP&Q* load models and therefore, causing a less direct relationship between load changes and node voltage variations. To elaborate further, in the constant *CP&Q* load models, the changes in the node voltage tend to be directly proportional to the changes in the load, which makes the voltage response more predictable and sensitive to variations in the load profile. On the other hand, in the ZIP load model, the response of the node voltage becomes less predictable and less proportional to the changes in the load, owing to the nonlinearity inherent in this model. The presence of MI provides additional pathways for power flow, influencing the voltage responses to variations in active power. This finding highlights the importance of considering MI in accurately assessing voltage sensitivity and optimizing the performance of the power distribution network.

3) IDENTIFICATION OF THE MOST SENSITIVE NODE WITH *"CP&Q AND ZIP LOAD WITH MI"*

To further explore the application of MI-based power flow analysis in identifying the most sensitive node in the DN, we conducted additional analysis. In this case, we considered the *"CP&Q and ZIP load with MI"* scenario and varied the power from 0 to 50 kW in a single step to evaluate the voltage variation. The results, as depicted in Figure 22, indicate
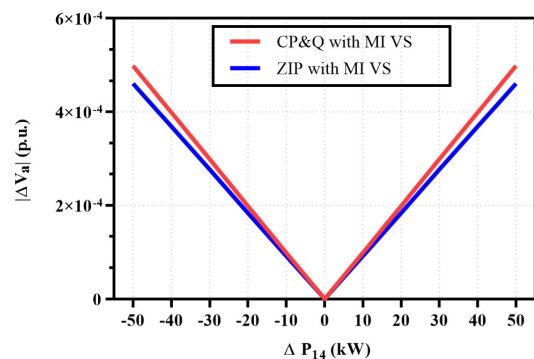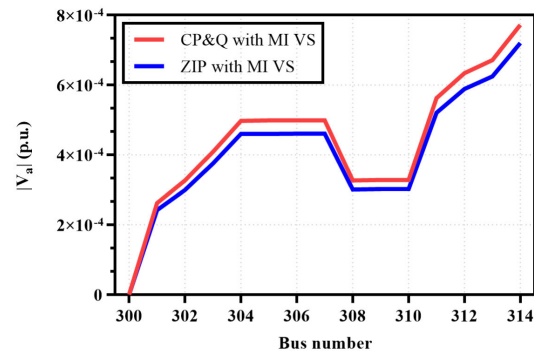
that nodes 11 to 14 exhibit higher voltage sensitivity in the *"CP&Q with MI"* case compared to the *"ZIP load with MI"* case.

VI. CONCLUSION

This paper addressed the challenges posed by intermittent power generation of DGs and highlights the importance of MI analysis in understanding the behavior of distribution lines, loads, and DGs in a DN. By incorporating MI analysis into the power flow problem formulation using the backward-forward sweep power flow mechanism and considering polynomial ZIP loads as well as DGs both with and without MI, this study provides significant technical insights that are essential for effective management and control of the power grid. The proposed model is applied to two case studies: the IEEE 34 bus test feeder and the KEPCO DN and the simulation results are varied using different scenarios. The results demonstrate the analysis of voltage profiles, system losses, voltage improvement, violations of nominal voltage limits, and voltage sensitivity, accounting for the temporal and spatial effects of loads and DG inductions. The findings underscore the significance of MI analysis in enhancing the operational efficiency and performance of power systems. Incorporating MI analysis enables power grid operators to gain deeper insights into the behavior of the DN, optimize voltage profiles, mitigate voltage fluctuations, and effectively plan for the integration of DGs, thereby contributing to a more resilient and reliable power grid in the presence of renewable energy sources and DGs.

In future research, the study will be extended to incorporate both the cost-benefit ratio of DGs and MI-based analysis, aiming to determine optimal locations for DGs. This expanded analysis will provide a more comprehensive understanding of the factors influencing DG placement decisions and further enhance the effectiveness of MI-based approaches in power grid management and planning.

REFERENCES

[1] C.-S. Karavas, K. Arvanitis, and G. Papadakis, "A game theory approach to multi-agent decentralized energy management of autonomous polygeneration microgrids," *Energies*, vol. 10, no. 11, p. 1756, Nov. 2017.

[2] J. F. P. Duque, M. T. V. Martinez, A. P. Hurtado, E. M. Carrasco, B. L. Sancho, K. F. Krommydas, K. A. Plakas, C. G. Karavas, A. S. Kurashvili, C. N. Dikaiakos, and G. P. Papaioannou, "Inter-area oscillation study of the Greek power system using an automatic toolbox," in *Proc. IEEE PES Innov. Smart Grid Technol. Eur. (ISGT Europe)*, Oct. 2021, pp. 1–6.

[3] Q. Peng and S. H. Low, "Distributed optimal power flow algorithm for radial networks, I: Balanced single phase case," *IEEE Trans. Smart Grid*, vol. 9, no. 1, pp. 111–121, Jan. 2018.

[4] D. Yu, S. Gao, X. Zhao, Y. Liu, S. Wang, and T. E. Song, "Alternating iterative power-flow algorithm for hybrid AC–DC power grids incorporating LCCs and VSCs," *Sustainability*, vol. 15, no. 5, p. 4573, Mar. 2023.

[5] W. F. Tinney and C. E. Hart, "Power flow solution by Newton's method," *IEEE Trans. Power App. Syst.*, vol. PAS-86, no. 11, pp. 1449–1460, Nov. 1967.

[6] B. Stott and O. Alsac, "Fast decoupled load flow," *IEEE Trans. Power App. Syst.*, vol. PAS-93, no. 3, pp. 859–869, May 1974.

[7] W. D. Stevenson, "Element of power system," in *Analysis*. New York, NY, USA: McGraw-Hill, 1975.

[8] A. H. El-Abiad and G. W. Stagg, *Computer Methods in Power System Analysis*. New York, NY, USA: McGraw-Hill, 1968.

[9] S. Iwamoto and Y. Tamura, "A load flow calculation method for ill-conditioned power systems," *IEEE Trans. Power App. Syst.*, vols. PAS–100, no. 4, pp. 1736–1743, Apr. 1981.

[10] D. Rajicic and A. Bose, "A modification to the fast decoupled power flow for networks with high R/X ratios," *IEEE Trans. Power Syst.*, vol. PS-3, no. 2, pp. 743–746, May 1988.

[11] W. Kersting, "A method to teach the design and operation of a distribution system," *IEEE Trans. Power App. Syst.*, vols. PAS–103, no. 7, pp. 1945–1952, Jul. 1984.

[12] R. Stevens, D. Rizy, and S. Purucker, "Performance of conventional power flow routines for real-time distribution automation applications," Oak Ridge Nat. Lab., Oak Ridge, TN, USA, Tech. Rep. CONF-860479-3 ON: DE86005587, 1986. [Online]. Available: https://www.osti.gov/biblio/6191841

[13] R. G. Cespedes, "New method for the analysis of distribution networks," *IEEE Trans. Power Del.*, vol. 5, no. 1, pp. 391–396, Jan. 1990.

[14] J.-H. Teng, "A network-topology-based three-phase load flow for distribution system," *Proc. Nat. Sci. Council, Republic China, A, Phys. Sci. Eng.*, vol. 24, no. 4, pp. 259–264, 2000.

[15] J.-H. Teng, "A direct approach for distribution system load flow solutions," *IEEE Trans. Power Del.*, vol. 18, no. 3, pp. 882–887, Jul. 2003.

[16] N. A. Rostami and M. O. Sadegh, "The effect of load modeling on load flow results in distribution systems," *Amer. J. Electr. Electron. Eng.*, vol. 6, no. 1, pp. 16–27, 2018.

[17] U. Eminoglu and M. H. Hocaoglu, "A new power flow method for radial distribution systems including voltage dependent load models," *Electric Power Syst. Res.*, vol. 76, nos. 1–3, pp. 106–114, Sep. 2005.

[18] S. Sunisith and K. Meena, "Backward/forward sweep based distribution load flow method," *Int. Elect. Eng. J. (IEEJ)*, vol. 5, no. 9, pp. 1539–1544, 2014.

[19] J. Yin, D. Lin, T. Parisini, and S. Y. Hui, "Front-end monitoring of the mutual inductance and load resistance in a series–series compensated wireless power transfer system," *IEEE Trans. Power Electron.*, vol. 31, no. 10, pp. 7339–7352, Oct. 2016.

[20] A. Rakhymbay, A. Khamitov, M. Bagheri, B. Alimkhanuly, M. Lu, and T. Phung, "Precise analysis on mutual inductance variation in dynamic wireless charging of electric vehicle," *Energies*, vol. 11, no. 3, p. 624, Mar. 2018.

[21] A. O. Mirzaei, A. M. Abazari, and H. Tavakkoli, "Investigating the effect of geometric design parameters on the mutual inductance between two similar planar spiral coils with inner and outer diameter limits," *J. Appl. Res. Electr. Eng.*, vol. 2, no. 1, pp. 70–74, 2023.

[22] H. Tavakkoli, E. Abbaspour-Sani, A. Khalilzadegan, G. Rezazadeh, and A. Khoei, "Analytical study of mutual inductance of hexagonal and octagonal spiral planer coils," *Sens. Actuators A, Phys.*, vol. 247, pp. 53–64, Aug. 2016.

[23] N. Helistö, J. Kiviluoma, H. Holttinen, J. D. Lara, and B. Hodge, "Including operational aspects in the planning of power systems with large amounts of variable generation: A review of modeling approaches," *WIREs Energy Environ.*, vol. 8, no. 5, p. e341, Sep. 2019.

[24] V. Boglou, C. Karavas, A. Karlis, K. G. Arvanitis, and I. Palaiologou, "An optimal distributed RES sizing strategy in hybrid low voltage networks focused on EVs' integration," *IEEE Access*, vol. 11, pp. 16250–16270, 2023.

[25] D. Rimpas, S. D. Kaminaris, D. D. Piromalis, G. Vokas, K. G. Arvanitis, and C.-S. Karavas, "Comparative review of motor technologies for electric vehicles powered by a hybrid energy storage system based on multi-criteria analysis," *Energies*, vol. 16, no. 6, p. 2555, Mar. 2023.

[26] M. Ali, M. F. Zia, and M. W. Sundhu, "Demand side management proposed algorithm for cost and peak load optimization," in *Proc. 4th Int. Istanbul Smart Grid Congr. Fair (ICSG)*, Apr. 2016, pp. 1–5.

[27] M. F. Zia, M. Nasir, E. Elbouchikhi, M. Benbouzid, J. C. Vasquez, and J. M. Guerrero, "Energy management system for a hybrid PV-wind-tidal-battery-based islanded DC microgrid: Modeling and experimental validation," *Renew. Sustain. Energy Rev.*, vol. 159, May 2022, Art. no. 112093.

[28] M. F. Zia, E. Elbouchikhi, and M. Benbouzid, "Optimal operational planning of scalable DC microgrid with demand response, islanding, and battery degradation cost considerations," *Appl. Energy*, vol. 237, pp. 695–707, Mar. 2019.

[29] S. Hussain, M. A. Ahmed, and Y.-C. Kim, "Efficient power management algorithm based on fuzzy logic inference for electric vehicles parking lot," *IEEE Access*, vol. 7, pp. 65467–65485, 2019.

[30] S. Hussain, K.-B. Lee, M. A. Ahmed, B. Hayes, and Y.-C. Kim, "Two-stage fuzzy logic inference algorithm for maximizing the quality of performance under the operational constraints of power grid in electric vehicle parking lots," *Energies*, vol. 13, no. 18, p. 4634, Sep. 2020.

[31] S. Hussain, S. Thakur, S. Shukla, Q. Jan, F. Khan, I. Ahmad, M. Marzband, and M. G. Madden, "A heuristic charging cost optimization algorithm for residential charging of electric vehicles," *Energies*, vol. 15, no. 4, p. 1304, Feb. 2022.

[32] S. Shukla, S. Thakur, S. Hussain, and J. G. Breslin, "A blockchain-enabled fog computing model for peer-to-peer energy trading in smart grid," in *Proc. Int. Congr. Blockchain Appl.* Cham, Switzerland: Springer, 2021, pp. 14–23.

[33] S.-H. Sohn, H.-S. Yang, J.-H. Lim, S.-R. Oh, S.-W. Yim, S.-K. Lee, H.-M. Jang, and S.-D. Hwang, "Installation and power grid demonstration of a 22.9 kV, 50 MVA, high temperature superconducting cable for KEPCO," *IEEE Trans. Appl. Supercond.*, vol. 22, no. 3, Jun. 2012, Art. no. 5800804.

[34] C. Kim Gan, N. Silva, D. Pudjianto, G. Strbac, R. Ferris, I. Foster, and M. Aten, "Evaluation of alternative distribution network design strategies," in *Proc. IET Conf. Publications*, 2009, pp. 1–4.

[35] C. S. Cheng and D. Shirmohammadi, "A three-phase power flow method for real-time distribution system analysis," *IEEE Trans. Power Syst.*, vol. 10, no. 2, pp. 671–679, May 1995.

[36] F. Calero, "Mutual impedance in parallel lines–protective relaying and fault location considerations," in *Proc. 34th Annu. Western Protective Relay Conf.*, Spokane, WA, USA, 2007, pp. 1–15.

[37] S. Hussain, S. Thakur, S. Shukla, J. G. Breslin, Q. Jan, F. Khan, and Y.-S. Kim, "A two-layer decentralized charging approach for residential electric vehicles based on fuzzy data fusion," *J. King Saud Univ. Comput. Inf. Sci.*, vol. 34, no. 9, pp. 7391–7405, Oct. 2022.

[38] S. Hussain, Y.-S. Kim, S. Thakur, and J. G. Breslin, "Optimization of waiting time for electric vehicles using a fuzzy inference system," *IEEE Trans. Intell. Transp. Syst.*, vol. 23, no. 9, pp. 15396–15407, Sep. 2022.

[39] S. Hussain, R. R. Irshad, F. Pallonetto, Q. Jan, S. Shukla, S. Thakur, J. G. Breslin, M. Marzband, Y.-S. Kim, M. A. Rathore, and H. El-Sayed, "Enhancing the efficiency of electric vehicles charging stations based on novel fuzzy integer linear programming," *IEEE Trans. Intell. Transp. Syst.*, pp. 1–15, May 2023, doi: 10.1109/TITS.2023.3274608.

[40] R. Zavadil, N. Miller, A. Ellis, and E. Muljadi, "Making connections [wind generation facilities]," *IEEE Power Energy Mag.*, vol. 3, no. 6, pp. 26–37, Nov. 2005.

[41] N. Srećković, *Optimization of the Distribution Network Operation by Integration of Distributed Energy Resources and Participation of Active Elements*. Maribor, Slovenia: Univerza v Mariboru, 2020.

[42] J. A. M. Rupa and S. Ganesh, "Power flow analysis for radial distribution system using backward/forward sweep method," *Int. J. Elect., Comput., Electron. Commun. Eng.*, vol. 8, no. 10, pp. 1540–1544, 2014.

[43] N. Nusrat, "Development of novel electrical power distribution system state estimation and meter placement algorithms suitable for parallel processing," Ph.D. dissertation, Dept. Electron. Elect. Eng., Brunel Univ. London, Uxbridge, U.K., 2015. [Online]. Available: https://bura.brunel.ac.uk/handle/2438/10902

[44] Q. Li, Y. Xu, C. Ren, and R. Zhang, "A probabilistic data-driven method for response-based load shedding against fault-induced delayed voltage recovery in power systems," *IEEE Trans. Power Syst.*, vol. 38, no. 4, pp. 3491–3503, Jul. 2023, doi: 10.1109/TPWRS.2022.3206839.

[45] S. Talkington, D. Turizo, S. Grijalva, J. Fernandez, and D. K. Molzahn, "Conditions for estimation of sensitivities of voltage magnitudes to complex power injections," *IEEE Trans. Power Syst.*, early access, pp. 1–14, Jan. 2023, doi: 10.1109/TPWRS.2023.3237505.

[46] G. Chagas and R. Pires, "The sequential power flow in complex plane for solving the VSC-MTDC hybrid AC/DC transmission grids," *Int. J. Electr. Power Energy Syst.*, vol. 148, Jun. 2023, Art. no. 108900.

[47] P. Shaw, "Modelling and analysis of an analogue MPPT-based PV battery charging system utilising DC–DC boost converter," *IET Renew. Power Gener.*, vol. 13, no. 11, pp. 1958–1967, Aug. 2019.

[48] S.-R. Nam, S.-H. Kang, J.-H. Lee, E.-J. Choi, S.-J. Ahn, and J.-H. Choi, "EMS-data-based load modeling to evaluate the effect of conservation voltage reduction at a national level," *Energies*, vol. 6, no. 8, pp. 3692–3705, Jul. 2013.

[49] J. Caballero-Peña, C. Cadena-Zarate, A. Parrado-Duque, and G. Osma-Pinto, "Distributed energy resources on distribution networks: A systematic review of modelling, simulation, metrics, and impacts," *Int. J. Electr. Power Energy Syst.*, vol. 138, Jun. 2022, Art. no. 107900.

[50] S. A. A. Kazmi, M. K. Shahzaad, and D. R. Shin, "Voltage stability index for distribution network connected in loop configuration," *IETE J. Res.*, vol. 63, no. 2, pp. 281–293, Mar. 2017.

[51] G. Hong and Y.-S. Kim, "Supervised learning approach for state estimation of unmeasured points of distribution network," *IEEE Access*, vol. 8, pp. 113918–113931, 2020.

[52] S. Impram, S. Varbak Nese, and B. Oral, "Challenges of renewable energy penetration on power system flexibility: A survey," *Energy Strategy Rev.*, vol. 31, Sep. 2020, Art. no. 100539.

[53] S. Ullah, A. M. A. Haidar, P. Hoole, H. Zen, and T. Ahfock, "The current state of distributed renewable generation, challenges of interconnection and opportunities for energy conversion based DC microgrids," *J. Cleaner Prod.*, vol. 273, Nov. 2020, Art. no. 122777.

[54] Y.-S. Kim, E.-S. Kim, and S.-I. Moon, "Frequency and voltage control strategy of standalone microgrids with high penetration of intermittent renewable generation systems," *IEEE Trans. Power Syst.*, vol. 31, no. 1, pp. 718–728, Jan. 2016.

SHAHID HUSSAIN received the B.S. degree in mathematics and the M.Sc. degree in computer science from the University of Peshawar, in 2002 and 2005, respectively, and the M.S. and Ph.D. degrees in computer engineering from Jeonbuk National University, South Korea, in 2016 and 2020, respectively. He was a Postdoctoral Researcher with the Gwangju Institute of Science and Technology (GIST), South Korea, in 2020, and the University of Galway (UoG), Ireland, from 2020 to 2022. He is currently a Senior Postdoctoral Researcher with the Innovation Value Institute (IVI), School of Business, National University of Ireland Maynooth (NUIM), Ireland. His current research interests include smart grids, energy management, electric vehicles, smart grid infrastructure, optimization algorithms, micro-grid operations, distributed energy resources, peer-to-peer energy trading, and machine learning in medical applications (e.g., prediction and risk analysis of osteoporosis) using fuzzy logic, game theory, ontology, AI, and blockchain approaches and technologies. He achieved the Jeonbuk National University Presidential Award for academic excellence during the Ph.D. studies.

JUNG-SUNG PARK received the B.S. and M.S. degrees in electrical engineering from Hongik University, Seoul, South Korea, in 2004 and 2006, respectively. He is currently pursuing the Ph.D. degree in power systems. He is currently a Senior Researcher with the Smart Power Distribution Laboratory, KEPCO Research Institute, Daejeon, South Korea. His current research interest includes to develop the policy and operation model of TSO-DSO coordination for virtual power plant (VPP) in distribution systems.

YUN-SU KIM (Senior Member, IEEE) received the B.S. and Ph.D. degrees in electrical engineering from Seoul National University, Seoul, South Korea, in 2010 and 2016, respectively. He was a Senior Researcher with the Korea Electrotechnology Research Institute (KERI), from 2015 to 2017. He joined the Faculty of the Gwangju Institute of Science and Technology (GIST), in 2018, where he is currently an Associate Professor with the Graduate School of Energy Convergence. His current research interests include distribution networks, distributed energy resources, microgrids, artificial intelligence, and wireless power transfer. He was the Director of the Korean Society for New and Renewable Energy and the Korean Institute of Electrical Engineers. He has been an Associate Editor of the IEEE Transactions on Sustainable Energy, since 2023.

EHTISHAM ASGHAR received the B.S. degree in electrical engineering from the University of Management and Technology (UMT), Lahore, Pakistan, in 2013, and the M.S. degree in control theory and control engineering from North China Electric Power University (NCEPU), Beijing, China, in 2018. He was a Research Assistant with the Gwangju Institute of Science and Technology (GIST), Gwangju, South Korea. His current research interests include microgrid operations, vehicle-to-grid technologies, battery swapping systems, integration of distributed energy resources, power system analysis, and power electronics.

REYAZUR RASHID IRSHAD received the B.Sc. degree from Aligarh Muslim University, Aligarh, India, in 2000, and the master's degree in computer application from Indira Gandhi University, New Delhi, India, in 2010. He is currently pursuing the Ph.D. degree with JJT University, Rajasthan. He is also a Lecturer with the Department of Computer Science, Najran University, Saudi Arabia. He has published many articles in reputed journals and has attended some conferences. His current research interest includes web-based applications.

● ● ●